Structure Based Virtual Screening of Rivastigmine Derivatives as Cholinesterase Inhibitors

Bhagirath Mandal
University of North Bengal
Syamantak Niyogi
University of North Bengal
Kaushik Sarkar
University of North Bengal
Rajesh Das (rajeshnbu@gmail.com)
University of North Bengal https://orcid.org/0000-0001-9433-4711

Research Article

Keywords: Alzheimer disease, rivastigmine, molecular docking, DFT, ADMET, molecular dynamics simulation

Posted Date: February 7th, 2022

DOI: https://doi.org/10.21203/rs.3.rs-1320847/v1

Abstract

The interaction of large protein molecules with small drug molecules is studied through *in silico* studies. The molecular docking and other important pharmacokinetic (ADMET) properties of the compounds were carried out with rivastigmine and its derivatives against protein Bovine Serum Albumin (PDB: 4F5S) to describe their better protein-ligand interactions and binding affinities. Rivastigmine is a promising drug that is used to treat Alzheimer disease. But due to the increased drug resistance property, its use becomes less effective. Hence, better drugs with higher potency are needed against this Alzheimer disease. In order to design a more potent drug computationally, we have taken here 52 derivatives of Rivastigmine and were docked against protein Bovine Serum Albumin. Besides, quantum chemical parameters like HOMO-LUMO bandgap energy and other important pharmacological analysis like ADMET studies were also carried out to predict better drug candidature. Molecular dynamics simulation and MMPBSA binding free energy calculations were also validated. From this computational study, 14 designed compounds were found to have better potency against Alzheimer disease.

Introduction

Nowadays, the discovery of new drugs for any disease and replacing old ones is a challenging task. Rivastigmine (Fig. 1) is a cholinergic drug and the use of cholinesterase inhibitors were began in 1997. Besides, various cholinergic drugs like rivastigmine, donepezil, and galantamine were used to treat Alzheimer's disease. Acetylcholine inhibitors also block acetylcholine esterase (AChE) which results in controlling Alzheimer disease [1]. In 2014, 5.3 million Americans suffered from Alzheimer disease. Acetylcholinesterase is an enzyme that hydrolyzes acetylcholine [2]. Rivastigmine patch is a transdermal treatment and was previously practiced for dementia of Alzheimer disease in the United States [3].

Alzheimer and Parkinson disease both damage the human brain. It can cause death of many cells in the human brain. As a result of this disease, effectivity of human vision is also greatly reduced. Although the human memory is fine at the beginning of the disease, gradually the memory decreases a lot, changes in human behavior can be noticed. Alzheimer disease causes behavioral changes in people and is treated with rivastigmine. Rivastigmine intake for a long time results in changes of the patient's behavior and mental state [4]. From 2000-2014, the death rate from Alzheimer disease was increased by 89% [3]. The problem of this disease has increases with age. The incidence of this disease doubles in every 5 years when the patient is 65 years old [5]. The incidence of Alzheimer's disease is higher after 65 years [6]. Alzheimer's disease is a brain disease and rivastigmine improves the brain function by enhancing human memory [7]. Once this disease starts, it gradually progresses and shows brain results in difficulty for the human body. People with this disease have higher difficulty for coordinating their various organs. Gradually it becomes difficult for people to speak and so people become nonsense.

In this study, various derivatives of rivastigmine were designed and docked against protein Bovine Serum Albumin (PDB: 4F5S). Through study, we would like to develop more advanced and highly effective drug compounds compared to rivastigmine to treat Alzheimer disease. Different data have been taken by changing the functional group in different positions of the Rivastigmine compound. Here, we have designed 52 new compounds followed by various useful analysis such as DFT, ADMET, molecular docking as well as molecular dynamics simulation and find out 14 best designed derivatives of Rivastigmine against Alzheimer disease.

Materials And Methods

Protein preparation

The three dimensional X-ray crystal structure of protein Bovine Serum Albumin was retrieved from the Protein Data Bank (PDB ID: 4F5S).Other chemical compounds were removed from the crystal structure of protein Bovine Serum Albumin prior to docking using Molegro Molecular Viewer (MMV)2.5.0 programme (CLC Bio, Qiagen Inc.).

Ligand preparation

All derivative ligand compounds along with the standard rivastigmine were drawn using ChemSketch Tool (ACD/Structure Elucidator, version 2018.1). The selected compounds having different substituents were shown in Table **1.** Preparation of ligands includes, adding all explicit hydrogens, 2D to 3D structure conversion. The molecules were optimized, using Density Functional Theory (DFT) [8, 9].

DFT study

Gaussian 09W [10] suite of software was used to minimize the energy search. Complete geometry optimization was done using DFT model restricted Becke's three parameters exchange potential and Lee-Yang-Parr correlation functional (RB3LYP) method and 6-31G(d,p) basis set [11, 12]. These best compounds with their optimized structures are shown in Fig. 2. Highest occupied molecular orbital (HOMO), lowest unoccupied molecular orbital (LUMO), energy gap, total minimum energy and dipole moment were calculated and shown in Table **2**.

ADME and toxicity parameters

PreADMET (http://preadmet.bmdrc.org/) server was used to test drug-likeness properties and ADME profiles (Absorption, Distribution, Metabolism, and Excretion) for all derived compounds. Molinspiration (http://www.molinspiration.com) and OSIRIS property explorer (http://www.organic-chemistry.org/prog/peo/) were also used to calculate various pharmacological parameters such as octanol-water partition coefficient (logP), solubility, topological polar surface area (TPSA), molecular weight (MW), drug-likeness, drug-score and number of violation to Lipinski's rule. The overall toxicity for most active derivative compounds was predicted by OSIRIS program as it indicates fragment based properties responsible for mutagenic, tumorigenic, irritant, and reproductive effect.

Molecular docking method

The docking protocol Autodock vina (ADT) [13] was used to predict the binding mode of rivastigmine and its derivatives into the binding site of protein Bovine Serum Albumin (PDB ID: 4F5S). The receptor molecule was prepared by adding all polar hydrogens with no bond order using graphical user interface of ADT. The ligands were also prepared as PDB format from all the optimized Gaussian output to assist rigid docking process. Active torsions were set to maximum number of atoms. Kollman charges have been assigned to the protein and Gasteiger charges to ligands. Pre-calculated grid map was required in ADT for each atom type in the ligand being docked to know the interacting potential energy by preparing grid box in such a way that it covered all the active site of amino acid residues prior to binding. The input grid box have size 50×40×50 Å (x, y and z) and center at -10.629, 13.455, 113.109 (x, y and z) with spacing 0.375 Å using Auto Grid 4.0, integrated in ADT. Lamarckian Genetic Algorithm (LGA) was kept as default in all separate molecular docking. The best docked models, with higher negative binding energies, were considered for further studies. All docking visualizations were performed using Discovery studio visualizer.

Molecular dynamics (MD) simulation

MD study using GROMACS 5.1.1 (http://www.gromacs.org/Downloads) was performed with the minimum energy conformers obtained after docking between proteins (PDB ID:4F5S) and two best designed compound (R36 and R47). Topology of protein was constructed in pdb2gmx using CHARMM36-jul2021 force-field [14] and TIP3P solvation model [15], while ligand topology was generated using CHARMM General Force Field server (CGenFF) [16, 17]. In this study, we used cubic periodic box setting a minimal distance of 1.0 nm between the protein and the edge of the box. All the protein moieties were neutralized by adding adequate number of ions. Using steepest descent algorithm and conjugate gradient protocol, energy minimization was performed until the maximum force of at least 10 kJ mol^{-1} nm^{-1}. Isochoric-isothermal (NVT) and isothermal-isobaric (NPT) ensembles were applied on the system for 100 ps for equilibration at 300Kby keeping 2-fs time step and 1.2 nm electrostatic and van der Waal cut-offs. Particle mesh Ewald (PME) [18] method was used for long range electrostatic interaction calculations. Finally, 10 ns MD simulation was subjected to the equilibrated ensembles with the same cut-offs. Various geometrical properties of the systems such as root mean square deviation (RMSD), root mean square

fluctuation (RMSF), solvent-accessible surface area (SASA) and radius of gyration were determined using gmx rmsd, gmx rmsf, gmx sasa and gmx gyrate programs. The graphs were plotted using Origin tool.

Binding free energy calculation by MMPBSA

In this present work, we have determined the molecular mechanics Poison–Boltzmann surface area(MM/PBSA) free binding energy between the proteins and ligands (R36 and R47) using g_mmpbsa tool [19, 20]. The MM-PBSA method allows us to estimate the free binding energy of complexation from molecular dynamics trajectories [21]. This method can be used in the application of virtual screens or docking to refine the classification of poses. In this technique, ΔG_{bind} is assessed from the free energies of the protein–ligand system in equation 1:

$$\Delta G_{bind} = G_{protein-ligand} - (G_{protein} + G_{ligand}) \quad (1)$$

The free energy for each individual entity is given by equation 2:

$$G_x = E_{MM} + G_{solv} - TS_{MM} \quad (2)$$

where, x denotes the protein or ligand or protein–ligand complex, E_{MM} is the molecular mechanics potential energy in vacuum, and G_{solv} is the free energy of solvation. Here, TS denotes to the entropic contribution to the free energy in vacuum, where T and S represent the temperature and entropy respectively.

The solvation free energy is the sum of polar and non-polar free energy:

$$G_{solv} = G_{polar} + G_{non-polar} \quad (3)$$

Here, E_{MM} contains the bonded and non-bonded interactions energy which comprise both electrostatic (E_{elec}) and van derWaals (E_{vdw}) interactions.

$$E_{MM} = E_{non-bonded} + E_{bonded} + (E_{vdw} + E_{elec}) \quad (4)$$

Results

It was shown from Table S1, that all the compounds used in this study were successfully qualified the Lipinski,s rule of five [22] and CMC like rule. Except few of them, most of these ligands were predicted to have good oral bioavailability (Table 3). A large number of compounds have shown excellent permeability, while few have relatively less or poor permeability (Table 4). The derived physical parameters like ionization potential (I), electron affinity (A), global hardness (η), softness (S), chemical potential (μ), electronegativity (σ), and electrophilicity (ω), play an important role to decide activity of these derived compounds (Table S2). The drug score and drug-likeness values for the ligands were also predicted and are shown in Table S3. It was revealed from the data that 27 compounds have drug score value, in the range of 0.5-0.95, and the rest of the compounds between 0.08-0.49.

Toxicity effect can predict the fate of a promising drug. It has been shown that drug molecules, having low toxicity/side effect, contain the high order of therapeutic index. So toxicity prediction was done for all the derived compounds, using OSIRIS Property Explorer (Table S4). It was noted that all the derived compounds, except few of them have higher or moderate toxicity. The toxicity parameters were used in OSIRIS as color codes, as usual, green stands for low, yellow stands formediocre, and red stands for high toxicity.The molecular docking results revealed that the docked complex of 23 derived compounds have higher negative binding energies (docked with PDB: 4F5S) compared to standard rivastigmine (-6.6 Kcal/mol) (Table **1**).

Discussion

DFT analysis

There are several ways, in which chemical stability of a molecule can be calculated. The simplest one involves difference in energy between highest occupied molecular orbital (HOMO) and lowest unoccupied molecular orbitals (LUMO) of a system. It is also a key parameter to determine the molecular properties of a molecule [22]. Energy of HOMO and LUMO are computed theoretically by DFT-RB3LYP/6-31G(d,p) method and the contour diagrams of best molecules are shown in Fig. 3, where positive and negative lobes are noted as red and green color, respectively. HOMO has ability to donate electron and behave as nucleophile and on the other hand, LUMO has electron accepting tendency from nucleophile, behave like electrophile [23].

The chemical reactivity, kinetic stability, optical polarizability and chemical hardness-softness of a molecule depend on the band gap energy (ΔE_{HL}) of HOMO and LUMO. Molecule possessing small ΔE_{HL}, has higher chemical reactivity as well as highly polarizable and behaves as soft molecule [24, 25]. On the other hand, relatively higher ΔE_{HL} value indicates high chemical stability as well as least chemical reactivity for a molecule. Besides, the molecules with higher dipole moment have a tendency to participate in strong intermolecular interaction. The chemical softness of the molecules depends on the degree of chemical reactivity and the reverse is in the case of hardness [26].

In this study, we have found 34 derived molecules with higher ΔE_{HL} value (> 5.65eV) and the remaining 19 compounds with low or slightly small ΔE_{HL} value (< 5.65eV). Among them, R9 has the highest value (8.5eV) and therefore it is highly unreactive species. On the other hand, R41 is the compound possessing the lowest ΔE_{HL} of 3.7eV and is considered as highly polarizable, reactive species i.e. soft compound. From dipole moment parameters, it is found that 7 compounds such as R8, R9, R15, R27, R35, R43 and R50 have larger tendency, to participate in strong intermolecular interaction (dipole moment > 6 Debye).

Global reactivity descriptors

In order to understand various aspects of pharmacological properties and eco-toxicological character of drug molecules, several new chemical descriptor parameters have been developed. Conceptual DFT based parameters were used to understand the structure, reactivity of molecules by calculating various useful parameters like chemical potential, global hardness, softness and electrophilicity index. Using HOMO and LUMO energy, the ionization potential (I) and electron affinity (A) can expressed as

$$I = -E_{HOMO} \quad (1)$$

$$A = -E_{LUMO} \quad (2)$$

Using these values, other descriptor properties such as chemical potential (μ), global hardness (η), global softness (S), electronegativity (σ) and electrophilicity index (ω) were calculated.

$$\mu = \frac{E_{LUMO}+E_{HOMO}}{2} \quad (3)$$

$$\eta = \frac{E_{LUMO}-E_{HOMO}}{2} \quad (4)$$

$$S = {}^{1}/_{\eta} \quad (5)$$

$$\sigma = -\mu \quad (6)$$

$$\omega = \frac{\mu^2}{2\eta} \quad (7)$$

Chemical stability of a system is represented by global hardness [24]. This property predicts the measure of resistance to change the distribution of electronic charge in a molecule [25]. According to Parr, electrophilicity index (ω) has determine the capacity of a species to accept electron [26]. The lower chemical hardness value (≤2.83eV) with low chemical potential

(μ<-2.74eV) of R13, R15, R27, R35, R36, R41, R44 and R45 may lead to act these compounds as soft with higher polarizablility, compared to others in this series. On the other hand, higher value of electronegativity (σ>3eV) and elecrophilicity index (ω>1.5eV) of R12, R15, R27,R28, R29, R35, R36, R41, R43, R44, R45, R46, R50 and R52 have indicated higher electron withdrawing tendency, act like electrophiles.

Molecular descriptor properties

In silico drug like properties and bioactive score were used to select best drug candidates, using OSIRIS suite and Molinspiration online property toolkit. Mutagonic, tumorigenic, irritant, reproductive index and drug-like, drug score values were visualized from OSIRIS and similarly, Molinspiration web server has predicted such valuable parameters like miLogP, TPSA, number of rotatable bonds (nrotb), number of hydrogen bond acceptors (nON) and donors (nOHNH). Good permeability across cell membrane is based on miLogP parameter. The tendency of generating hydrogen bonds is based on TPSA parameter. Number of rotatable bonds denotes the flexibility of a molecule. Molecular properties and structural features, irrespective of known drugs were checked on the basis of drug-likeness data of molecules [27]. The excellent results (Table 3, S3, S4) have shown the probability of these compounds as future drugs.

According to Lipinski's rule of five, all compounds having zero violation have shown good bioavailability and here all the derived compounds may act as good bioavailable drug. Molecules having nOHNH≤5, have indicated higher probability of solubility in cellular membranes and here all of these derived compounds have followed this rule [28]. Besides, all the molecules having molecular weight, MW<450, nON≤10, nrotb<10 and TPSA<160Å, are qualified oral route of newly designed molecules [29, 30].

ADME Prediction

Table 4 illustrates the *in silico* ADME properties. Most important parameters, used for pharmacokinetic study of a drug are absorption, distribution, metabolism and excretion [31]. In silico ADME properties of most of these derived compounds have shown satisfactory result. In this present work, 34 derived compounds have better result for intestinal absorption (HIA>90%), closed to 100. Out of these, R19 containing highest value of HIA (100%), has shown maximum absorption. Most of the derived compounds have followed moderate permeability in vitro Caco2 cell ranges, 19-22 nm/sec and few of them were failed, showing very unsatisfactory results. Also they have low or moderate permeability for in vitro MDCK cells. Results having, in vivo blood brain barrier (BBB) penetration indicate that most of the compounds (except R3, R20 and R44) have low absorption into central nervous system (CNS), less capability to cross CNS. 23 compounds, containing plasma protein binding data (PPB) indicate higher bound capacity, higher skin permeability than standard rivastigmine. Thus from overall results, we may concluded that most of these derived compounds have capability of good drug likeness and ADME properties.

Molecular docking studies

Molecular docking is becoming an increasingly significant method to realize the foundation of protein-ligand visualization [32].This present study was done to determine the binding affinity of the ligands with the active sites of bovine serum albumin (PDB: 4F5S) (Table S5). Binding energy of a protein-ligand complex gives the idea of strength and affinity of the interaction between the ligand and the protein. Binding energy of rivastigmine has shown the value of -6.6Kcal/mol when docked with receptor. The docking results indicated that 23 derived compounds have better results of binding energy than standard rivastigmine as shown in Fig. 4. These best 23 compounds are named as R1, R2, R3, R4, R5, R6, R8, R10, R13, R22, R24, R27, R28, R30, R32, R36, R40, R42, R45, R47, R49, R50 and R53. Among them, binding energies of the compounds R36 and R47 were come out as highest (-7.6 Kcal/mol and -7.5 Kcal/mol respectively). The active site residues of the receptor was represented as ASP323, ARG208, LEU326, LYS350, ALA212, ALA349, GLU353, ALA209, LEU346, LEU480, PHE205, VAL481, LEU330, GLY327, LYS211. Introduction of two acid groups (-COOH) in R36 compound (Fig. 5) and one amide group ($-CONH_2$) in R47 compound (Fig. 6) have given the highest value of negative binding energy. From the docking result we found one conventional hydrogen bond for compounds R2, R1,R12,R18, R20,R26, R32, R28, R36 R37, R45, R52 ; two

conventional hydrogen bonds for compounds R7, R9, R13,R19, R21, R23, R30, R43, R50, R53; three conventional hydrogen bonds for R3, R8, R10, R29, R34, R35, R37, R38, R40, R47.

MD simulation analysis

The best protein-ligand complexes of the receptor (PDB ID: 4F5S) docked with two best designed inhibitors (R36 and R47) along with standard rivastigmine were simulated for understanding structural deviations in dynamic environment for the time scale of 10 ns. Each inhibitor along with its complex was recorded for root mean square deviation (RMSD) from its initial position and the calculated values were plotted in **Fig. 7a**. It has been found that the RMSD of these compounds shows satisfactory stability in dynamic conditions.

In this case, RMSD lines for all the two docked complexes have follow the similar pattern and are almost coincide with the standard protein-rivastigmine complex line. All these three lines are parallel to x-axis after 2 ns. In case of ligands cases, these best designed docked compounds (R36 and R47) have lower RMSD pattern, compared to standard rivastigmine after approximately 4 ns In conclusion, all these two ligands have satisfied the validation of protein-ligand interactions in terms of RMSD values. In **Fig. 7b**, we have shown the root mean square fluctuation (RMSF), which measures the deviation of each amino acid of the used protein over a time interval of 10 ns. The overall result shows that the RMSF values of all the amino acids of the proteins docked with these two best inhibitors along with standard one do not change considerably as compared to their receptors.

On the other hand, Fig. S1 illustrates the radius of gyration (Rg) and solvent accessible surface area (SASA) plots for these two best ligands along with standard rivastigmine, docked with studying receptors. Rg has determined the compactness of the system. Both these complexes correspond similar Rg pattern of about 2.78 nm as compared to standard complex after 10 ns, revealing similar compact behaviour for these two complexes (Fig. S1a). In Fig. S1b, it has been found that the docked structures (protein-R36 and protein-R47) have almost similar SASA pattern of around 303 nm^2, compared with protein-rivastigmine complex.

Furthermore, we have performed g_mmpbsa binding free energy analysis and we have measured the contribution energy of each residues as shown in Fig. S2. Different free energy parameters that contribute to the binding energy are plotted in Fig. 8. Here, the docked complex of R47-4F5S has the highest contribution towards van der Waal interaction, electrostatic, polar and non-polar solvation as well as binding free energy (Table S5).

Conclusion

In summary, 52 derivative analogs of rivastigmine have been theoretically investigated against Alzheimer disease. This systematic study has been carried out in three different parts: (1) electronic and quantum mechanical study of compounds using DFT at RB3LYP level of 6-3G(d,p) basis set, (2) molecular docking study of each molecule in the active site of bovine serum albumin, (3) drug-likeness and toxicity prediction and comparing its results with standard drug rivastigmine. Comparative docking study of 9 molecules have shown that R3, R4, R6, R8, R10, RA22, R24, R27 and R42 have considerable binding energy, but fail to act like drug because of usual deviation from quantum mechanical parameters (high band gap, low softness), drug-likeness and toxicity parameters.

Considering quantum mechanical and electronic properties obtained from DFT, molecular docking studies and also drug-likeness, toxicity parameters have shown that 14 analogs such as R1, R2, R5, R13, R28, R30, R32, R36, R40, R45, R47, R49, R50 and R53 have been predicted to be more chemically reactive, good drug-like behavior, contain low toxicity with higher absolute value of ligand binding energies. In conclusion, these 14 analogs could be considered as lead molecules to enhance their therapeutic index by enhancing interactions with the target protein.

Declarations

Conflicts of interest

The authors declare no conflict of interest.

Acknowledgements

Authors are thankful to Department of Chemistry, University of North Bengal for various supports to do this wonderful research.

References

1. Babitha PP, Sahila MM, Bandaru S, Nayarisseri A, Sureshkumar SJB (2015) Molecular Docking and pharmacological investigations of rivastigmine-fluoxetine and coumarin–tacrine hybrids against acetyl choline esterase. 11:3788
2. Ali MR, Sadoqi M, Møller SG, Boutajangout A, Mezei, MJJoMG (2017) Modelling Assess binding cholinesterase inhibitors docking Mol dynamics Stud 76:36–42
3. Khoury R, Rajamanickam J, Grossberg, GTJTaids (2018) An update on the safety of current therapies for Alzheimer's disease: focus on rivastigmine. 9:171–1783
4. Rösler M, Retz W, Retz-Junginger P, Dennler HJJBN (1998) Effects of two-year treatment with the cholinesterase inhibitor rivastigmine on behavioural symptoms in Alzheimer's disease. 11:211–2164
5. Querfurth HW, LaFerla FMJNEJM (2010) Mech disease 362(4):329–344
6. Long JM, Holtzman DMJC (2019) Alzheimer disease: an update on pathobiology and treatment strategies. 179:312–3392
7. Bacalhau P, San Juan AA, Goth A, Caldeira AT, Martins R, Burke AJJBc (2016) Insights into (S)-rivastigmine inhibition of butyrylcholinesterase (BuChE): Molecular docking and saturation transfer difference NMR (STD-NMR). 67:105–109
8. Levy MJTieg. Density Functional Methods in Physics (1985) :32-94
9. Parr RG (1980) Density functional theory of atoms and molecules. Horizons of quantum chemistry. Springer, pp 5–15
10. Frisch M, Trucks G, Schlegel HB, Scuseria GE, Robb MA, Cheeseman JR et al (2009) gaussian 09, Revision d. 01, Gaussian. ;201
11. Stephens PJ, Devlin FJ, Chabalowski CF, Frisch MJJTJopc (1994) Ab initio calculation of vibrational absorption and circular dichroism spectra using density functional force fields. 98:11623–1162745
12. Lee C, Yang W, Parr RGJPrB (1988) Development of the Colle-Salvetti correlation-energy formula into a functional of the electron density. 37:7852
13. Trott O, Olson AJJJocc (2010) AutoDock Vina: improving the speed and accuracy of docking with a new scoring function, efficient optimization, and multithreading. 31:455–4612
14. Lee S, Tran A, Allsopp M, Lim JB, Hénin J (2014) Klauda JBJTjopcB. CHARMM36 united atom chain model for lipids and surfactants. ;118(2):547-56
15. Boonstra S, Onck PR, van der Giessen EJTjopcB (2016) CHARMM TIP3P water model suppresses peptide folding by solvating the unfolded state. 120:3692–369815
16. Vanommeslaeghe K, Hatcher E, Acharya C, Kundu S, Zhong S, Shim J et al (2010) CHARMM general force field: A force field for drug-like molecules compatible with the CHARMM all-atom additive biological force fields. 31:671–6904
17. Vanommeslaeghe K, MacKerell Jr (2012) ADJJoci, modeling. Automation of the CHARMM General Force Field (CGenFF) I: bond perception and atom typing. 52:3144–315412
18. Abraham MJ, Gready JEJJocc (2011) Optimization of parameters for molecular dynamics simulation using smooth particle-mesh Ewald in GROMACS 4.5. 32:2031–20409
19. Kumari R, Kumar R, Consortium OSDD (2014) Lynn AJJoci, modeling. g_mmpbsaî—¸ A GROMACS tool for high-throughput MM-PBSA calculations. 54:1951–19627

20. Baker NA, Sept D, Joseph S, Holst MJ, McCammon JAJPotNAoS (2001) Electrostatics of nanosystems: application to microtubules and the ribosome. 98:10037–1004118
21. Kollman PA, Massova I, Reyes C, Kuhn B, Huo S, Chong L et al (2000) Calculating structures and free energies of complex molecules: combining molecular mechanics and continuum models. 33:889–89712
22. Sarkar K, Das RKJIJoCB, Design D (2021) Molecular docking, ADME and toxicity study of some chemical and natural plant based drugs against COVID-19 main protease. 14:43–631
23. Reed JLJTJoPCA (1997) Electronegativity: chemical hardness I. 101:7396–740040
24. Barim E, Akman FJJoMS (2019) Synthesis, characterization and spectroscopic investigation of N-(2-acetylbenzofuran-3-yl) acrylamide monomer: Molecular structure, HOMO–LUMO study, TD-DFT and MEP analysis. 1195:506–513
25. Pauling LJI (1960) NY. The nature of the chemical bond and the structure of molecules and crystals: an introduction to modern structural chemistry.
26. Parr RG, Yang WJJotACS (1984) Density functional approach to the frontier-electron theory of chemical reactivity. 106:4049–405014
27. Lipinski CA, Lombardo F, Dominy BW, Feeney PJJAddr (1997) Experimental and computational approaches to estimate solubility and permeability in drug discovery and development settings. 23:3–251-3
28. Husain A, Ahmad A, Khan SA, Asif M, Bhutani R, Al-Abbasi FAJSPJ (2016) Synthesis, molecular properties, toxicity and biological evaluation of some new substituted imidazolidine derivatives in search of potent anti-inflammatory agents. 24:104–1141
29. Sarkar K (2021) Das RKJJoCB, Chemistry. In Silico study of Rosmarinic Acid Derivatives as Novel. Insulin Fibril Inhibitors 20(06):641–654
30. Sarkar K, Sarkar S, Das RKJCC-ADD (2021) Screening of Drug Efficacy of Rosmarinic Acid Derivatives as Aurora Kinase Inhibitors by Computer-Aided. Drug Des Method 17(5):627–646
31. Lee S, Lee I, Kim H, Chang G, Chung J, No KJEDD et al (2003) The PreADME Approach: Web-based program for rapid prediction of physico-chemical, drug absorption and drug-like properties. 2003:418–420
32. Ding F, Peng WJMB (2015) Biological activity of natural flavonoids as impacted by protein flexibility: an example of flavanones. 11:1119–11334

Tables

Table 1 Compounds having different substituents of Rivastigmine and its binding energy.

Compounds	Substituted groups	Substituted by	$\Delta G_{Binding}$ (Kcal/mol)
Rivastigmine	-	-	-6.6
R1	10-H	10-OH	-7.2
R2	11-H	11-OH	-7.0
R3	10-H	10-COOH	-6.7
R4	10-H	10-$CONH_2$	-6.8
R5	11-H	11-NH_2	-6.9
R6	4-CH_3	4-OH	-7.0
R7	10-H, 4-CH_3	10-OH, 4-OH	-6.2
R8	4-CH_3	4-NO_2	-7.0
R9	4-CH_3, 10-H	4-OH, 10-NO_2	-6.3
R10	10-H, 4-CH_3	10-COOH, 4-OH	-7.0
R11	10-H, 11-H	10-OH, 11-$CONH_2$	-6.0
R12	10-H, 11-H	10-OH, 11-OH	-6.3
R13	4-CH_3, 3-CH_3	4-OH, 3-OH	-7.0
R14	1-H	1-NH_2	-6.5
R15	10-H, 4-CH_3, 17-H	10-NO_2, 4-OH, 17-OH	-6.1
R16	2-H, 1-H	2-NH_2, 1-OH	-6.6
R17	1-H, 2-H	1-OH, 2-OH	-6.6
R18	1-H, 2-H	1-NH_2, 2-NH_2	-6.4
R19	13=O	13-OCH_3	-5.3
R20	10-H	10-OCH_3	-6.3
R21	10-H, 11-H	10-OCH_3, 11-NH_2	-6.1
R22	1-H, 2-H, 10-H	1-OH, 2-NH_2, 10-OH	-6.7
R23	1-H, 10-H, 11-H	1-OH, 10-OH, 11-OH	-6.4
R24	1-H,2-H, 10-H	1-OH, 2-OH, 10-OH	-6.7
R25	8-H, 10-H, 9-H	8-OH, 10-NH_2, 9-OH	-6.3
R26	10-H, 11-H	10-NH_2,11-NH_2	-6.3
R27	10-H, 4-CH_3	10-COOH, 4-OH	-6.7
R28	16-H, 4-CH_3	16-OH, 4-OH	-7.1

R29	16-H, 10-H	16-OH, 10-OH	-6.4
R30	17-H, 4-CH_3	17-COOH, 4-OH	-7.1
R31	10-H, 17-H	10-CH_3 17-COOH	-6.4
R32	10-H, 16-H	10-CH_3, 16-CH_3	-6.7
R33	10-H, 5-H	10-CH_2OH, 5-OH	-5.6
R34	10-H, 17-H	10-OH, 17-COOH	-6.5
R35	10-H, 17-H	10NO_2, 17-COOH	-6.0
R36	10-H, 17-H	10-COOH, 17-COOH	-7.6
R37	10-H, 17-H	10-OH, 17-COOH	-6.4
R38	10-H, 17-H	10-OH, 17-NH_2	-5.7
R39	10-H, 17-H	10-NH_2, 17-NH_2	-6.0
R40	10-H, 17-H, 4-CH_3	10-NH_2,17-COOH, 4NH_2	-6.7
R41	10-H, 17-H	10-NH_2, 17NO_2	-6.5
R42	17-H, 1-H	17-COOH, 1-OH	-7.0
R43	17-H, 1-H	17-OH, 1-COOH	-6.5
R44	1-H	1-CHO	-6.6
R45	17-H	17-CHO	-6.9
R46	1-H, 17-H	1-CHO, 17-CHO	-6.3
R47	1-H	1-$CONH_2$	-7.5
R48	1-H, 17-H	1-$CONH_2$, 17-$CONH_2$	-6.4
R49	17-H	17-$CONH_2$	-6.7
R50	1-H	1-COOH	-6.8
R52	1-H	1-F	-6.6
R53	17-H	17-OH	-6.9

Table 2 Calculated energy values of Rivastigmine and its derivatives using RB3LYP/6-31G(d,p) basis set

Molecule	E_{HOMO} (eV)	E_{LUMO} (eV)	ΔE_{HL} (Band gap) (eV)	Energy (eV)×10^{-4}	Dipole Moment (Debye)
Rivastagmine	-5.57	0.09	5.65	-2.20	2.85
R1	-5.64	0.06	5.70	-2.40	2.87
R2	-5.29	0.04	5.33	-2.40	3.62
R3	-6.00	1.26	7.26	-2.71	4.84
R4	-5.84	0.90	6.75	-2.65	3.23
R5	-5.34	0.27	5.61	-2.35	3.87
R6	-6.00	0.04	6.04	-2.29	3.32
R7	-6.00	0.18	6.18	-2.50	1.07
R8	-6.47	1.68	8.15	-2.64	6.20
R9	-6.35	2.14	8.50	-2.85	8.07
R10	-6.08	1.15	7.22	-2.81	3.03
R11	-5.72	0.06	5.77	-2.86	4.61
R12	-5.25	0.07	5.32	-2.60	2.77
R13	-5.82	-0.40	5.42	-2.39	3.68
R14	-5.73	0.13	5.85	-2.35	3.34
R15	-6.27	-2.20	4.07	-3.05	6.26
R16	-5.94	0.09	6.04	-2.55	3.75
R17	-5.90	0.06	5.96	-2.60	4.49
R18	-5.69	0.12	5.81	-2.50	2.05
R19	-5.69	0.12	5.81	-2.31	1.08
R20	-5.65	0.14	5.79	-2.51	2.83
R21	-4.87	0.24	5.11	-2.66	3.45
R22	-5.85	0.03	5.89	-2.76	2.19
R23	-5.30	0.01	5.31	-2.81	3.94
R24	-5.79	0.09	5.89	-2.81	4.36
R25	-5.36	0.29	5.65	-2.76	3.99
R26	-4.64	0.31	4.96	-2.50	2.49
R27	-6.06	-1.17	4.89	-2.81	8.17
R28	-5.96	-0.16	5.80	-2.50	2.3762
R29	-5.80	0.07	5.87	-2.60	2.0027
R30	-6.00	-0.22	5.77	-2.81	1.727

R31	-5.73	0.05	5.78	-2.82	2.5194
R32	-5.70	0.14	5.83	-2.41	2.542
R33	-5.33	0.21	5.53	-2.71	0.7392
R34	-5.83	0.01	5.84	-2.91	2.9496
R35	-6.00	-2.27	3.73	-3.26	8.437
R36	-5.73	-1.25	4.48	-3.22	3.3553
R37	-5.83	0.01	5.84	-2.91	2.9502
R38	-5.71	0.14	5.85	-2.55	2.2473
R39	-5.33	0.23	5.56	-2.50	0.8264
R40	-5.46	0.02	5.49	-2.90	3.8067
R41	-5.53	-1.83	3.70	-2.90	4.2946
R42	-5.94	-0.04	5.89	-2.91	3.2099
R43	-6.13	-0.14	5.99	-2.91	6.9339
R44	-6.17	-0.69	5.49	-2.50	4.9539
R45	-5.71	-0.64	5.07	-2.50	3.2332
R46	-6.28	-0.86	5.42	-2.81	4.0118
R47	-5.79	0.11	5.90	-2.65	5.5286
R48	-5.82	0.05	5.87	-3.11	3.1368
R49	-5.76	0.04	5.80	-2.65	1.9587
R50	-6.08	-0.03	6.05	-2.71	6.696
R52	-6.22	-0.01	6.20	-2.47	2.204
R53	-5.77	0.02	5.80	-2.40	2.0585

Table 3 Pre-ADMET Prediction of Rivastigmine and compounds.

Compounds	miLogP	TPSA[a]	Natoms[b]	nON[c]	nOHNH[d]	n-violations[e]	nrotb[f]	volume
Rivastigmine	2.28	32.78	18	4	0	0	5	254.01
R1	1.75	53.01	19	5	1	0	5	262.03
R2	1.79	53.01	19	5	1	0	5	262.03
R3	2.14	70.08	21	6	1	0	6	281.01
R4	1.05	75.88	21	6	2	0	6	284.29
R 5	1.69	58.80	19	5	2	0	5	265.30
R6	1.25	53.01	18	5	1	0	5	245.47
R7	0.73	73.24	19	6	2	0	5	253.49
R8	1.67	78.61	20	7	0	0	6	260.79
R9	1.17	98.83	21	8	1	0	6	268.81
R10	1.12	90.31	21	7	2	0	6	272.47
R11	0.50	96.10	22	7	3	0	6	292.30
R12	1.26	73.24	20	6	2	0	5	270.05
R13	0.94	73.24	18	6	2	0	5	236.93
R14	1.67	58.80	19	5	2	0	6	265.54
R15	0.16	119.06	22	9	2	0	7	277.06
R16	1.03	79.03	20	6	3	0	7	273.80
R17	0.99	73.24	20	6	2	0	7	270.53
R18	1.07	84.83	20	6	4	0	7	277.07
R19	2.69	24.94	19	4	0	0	7	277.40
R20	2.29	42.02	20	5	0	0	6	279.56
R21	1.70	68.04	21	6	2	0	6	290.85
R22	0.50	99.26	21	7	4	0	7	281.82
R23	0.62	93.47	21	7	3	0	6	278.31
R24	0.46	93.47	21	7	3	0	7	278.55
R25	0.93	99.26	21	7	4	0	5	281.34
R26	0.71	84.83	20	6	4	0	5	276.59
R27	1.12	90.31	21	7	2	0	6	272.47
R28	0.60	73.24	19	6	2	0	5	253.51
R29	1.09	73.24	20	6	2	0	5	270.80
R30	0.40	90.31	21	7	2	0	7	272.71
R31	1.82	70.08	22	6	1	0	7	297.82

R32	2.97	32.78	20	4	0	0	5	287.16
R33	0.56	73.24	21	6	2	0	7	287.09
R34	0.89	90.31	22	7	2	0	7	289.27
R35	1.33	115.90	24	9	1	0	8	304.59
R36	1.28	107.38	24	8	2	0	8	308.26
R37	0.89	90.31	22	7	2	0	7	289.27
R38	0.18	79.03	20	6	3	0	6	273.56
R39	-0.27	84.83	20	6	4	0	6	276.83
R40	-0.53	122.13	22	8	5	0	7	287.27
R41	0.71	104.63	22	8	2	0	7	288.88
R42	0.77	90.31	22	7	2	0	8	289.51
R43	-40	90.31	22	7	2	0	8	289.51
R44	2.10	49.85	20	5	0	0	7	273.24
R45	1.99	49.85	20	5	0	0	7	273.24
R46	1.81	66.92	22	6	0	0	9	292.46
R47	1.01	75.88	21	6	2	0	7	284.53
R48	-0.37	118.97	24	8	4	0	9	315.04
R49	0.90	75.88	21	6	2	0	7	284.53
R50	0.61	70.08	21	6	1	0	7	281.26
R52	2.56	32.78	19	4	0	0	6	259.19
R53	1.27	53.01	19	5	1	0	6	262.27

[a]Total polar surface area

[b] Number of heavy atoms present in the compound

[c]Number of hydrogen bond acceptors

[d]Number of hydrogen bond donors

[e]Number of violations made by proposed drug

[f]Number of rotatable bonds

Table 4 Molecular descriptor properties of Rivastigmine and compounds

Compounds	BBB	CaCO2	HIA	MDCK	PPB	Skin permeability	SKlogP value	SKlogS pure
Rivastigmine	1.16217	47.5911	99.415222	43.566	26.387634	-1.968	2.620070	-1.800070
R1	0.499828	27.361	95.119652	47.5221	34.060016	-2.5506	2.273920	-1.319270
R2	0.507105	29.2917	95.115064	62.7858	33.642588	-2.59927	2.539070	-1.076470
R3	1.16082	19.9862	96.066886	42.0786	26.083634	-2.88804	2.592610	-1.790450
R4	0.666831	19.4172	95.385400	27.9297	18.646095	-3.25799	1.728410	-1.932350
R5	0.669878	21.96	96.195048	43.743	23.243336	-2.72291	1.825690	-1.528760
R6	0.495142	19.2016	95.111338	70.6454	12.421550	-2.51509	1.792560	-1.361780
R7	0.437329	10.2587	90.104534	60.51	16.408142	-3.23631	1.446410	-0.880980
R8	0.522462	21.9088	92.270924	42.9023	25.620331	-2.97609	2.382270	-2.256620
R9	0.501965	1.49523	80.855977	59.0592	19.155872	-3.25437	1.877420	-2.007030
R10	0.437649	15.9586	87.226666	37.3769	15.569182	-3.43019	1.765100	-1.352160
R11	0.438217	16.4177	88.655356	14.3511	28.479049	-3.63106	1.112830	-1.227450
R12	0.616661	16.5458	90.651850	42.7282	37.625648	-3.21151	2.192920	-0.595670
R13	0.103843	20.8027	89.368589	26.6141	41.022845	-3.20828	0.530620	-1.342440
R14	0.0175174	21.5801	96.324029	45.3978	17.225652	-2.67788	2.066780	-2.567500
R15	0.216284	1.0979	60.525925	10.4341	17.358162	-3.51279	0.967660	-1.486850
R16	0.023832	20.4741	91.905337	26.0719	13.886587	-3.42818	1.188110	-1.989880
R17	0.0676393	20.7256	91.061282	35.2926	15.675083	-3.33625	0.862730	-0.644830
R18	0.0115219	19.8136	91.885510	16.8589	9.310493	-3.46535	1.513490	-2.807300
R19	0.829462	56.2171	100.00000	17.1875	11.821660	-1.82551	2.770300	-0.652860
R20	1.54009	53.0033	98.212480	42.5929	40.593344	-2.37801	2.654010	-1.963580
R21	0.751316	25.7969	96.221207	33.4496	33.039835	-3.21072	1.859630	-1.692270
R22	0.0389897	18.9313	81.985830	11.9988	14.092063	-3.83406	0.841960	-1.509080
R23	0.092552	17.6572	81.250329	19.9822	24.712115	-3.82289	1.314250	-0.018050
R24	0.0666676	19.6561	81.496460	20.134	15.205758	-3.85747	0.516580	-0.164030
R25	0.348447	11.0529	82.438500	11.845	28.047205	-3.82667	1.801770	-0.304140
R26	0.391698	17.8026	92.716853	11.6194	22.260921	-3.44883	1.201830	-1.461090
R27	0.437649	15.9586	87.226666	37.3769	15.569182	-3.43019	1.765100	-1.352160
R28	0.0492421	13.7065	90.294917	36.9091	13.047045	-3.34158	1.193290	-1.059190
R29	0.0858579	20.8544	90.860353	32.6935	29.966602	-3.33997	1.674650	-1.016680
R30	0.0103935	16.7608	87.226666	69.3047	14.297849	-3.30426	1.254540	-0.916790
R31	0.0147745	21.0226	96.724100	5.54605	33.951423	-2.88478	2.646100	-1.859310

R32	0.820849	50.427	99.263889	28.2848	41.023275	-1.91623	3.555460	-2.528110
R33	0.0572076	21.5686	91.695589	7.05786	15.973843	-3.55755	1.265000	-1.138680
R34	0.0196515	17.419	88.868483	29.4785	30.463008	-3.31133	1.735900	-0.874280
R35	0.0136545	6.80734	73.290720	1.34827	31.172896	-3.08256	2.166910	-2.000330
R36	0.0102649	18.9216	82.599427	2.00461	25.521346	-3.39524	2.054590	-1.859410
R37	0.0196515	17.419	88.868483	29.4785	30.463008	-3.31133	1.735900	-0.874280
R38	0.0282392	15.7963	91.516824	16.307	9.886880	-3.47194	1.273200	-1.206700
R39	0.0265201	17.8075	92.198461	5.69546	8.974546	-3.55301	0.995290	-1.619830
R40	0.033625	16.677	70.475794	38.0002	9.874006	-3.75078	0.539520	-1.784360
R41	0.0100495	4.89886	83.352323	19.9618	31.814022	-3.25208	1.675960	-2.107060
R42	0.0119574	20.0217	88.920167	37.7191	21.333873	-3.25866	1.203380	-0.777460
R43	0.246817	20.9853	88.922998	14.9907	32.491560	-3.34696	1.455460	-1.174340
R44	1.3459	33.3222	98.177825	68.7048	35.822287	-2.80881	2.065860	-1.855320
R45	0.0197157	29.4287	98.177825	33.4097	24.958010	-2.65353	1.782690	-1.515880
R46	0.197904	24.0667	97.828588	19.136	30.396077	-3.08897	1.228480	-1.571130
R47	0.108342	21.9242	95.376772	22.9231	28.468806	-3.22977	1.501020	-1.836420
R48	0.0296498	20.4505	82.663091	16.5803	13.656903	-3.50769	0.098800	-1.533330
R49	0.0111783	19.677	95.376894	38.8877	19.200908	-3.1864	1.217850	-1.496980
R50	0.922122	22.3153	96.066886	43.4705	39.656796	-3.054	2.365220	-1.694520
R52	0.0749711	31.5965	99.409326	34.7564	27.195640	-2.43243	3.007740	-2.385980
R53	0.0647141	23.3141	95.302478	42.2241	27.981614	-2.77693	1.710310	-1.279890

Figures

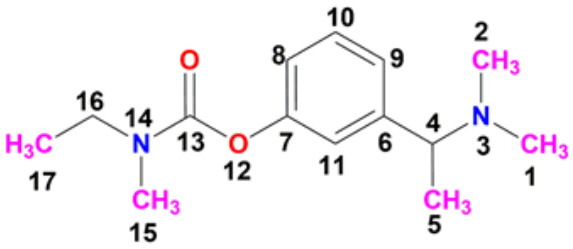

Figure 1

Chemical Structures of rivastigmine drug

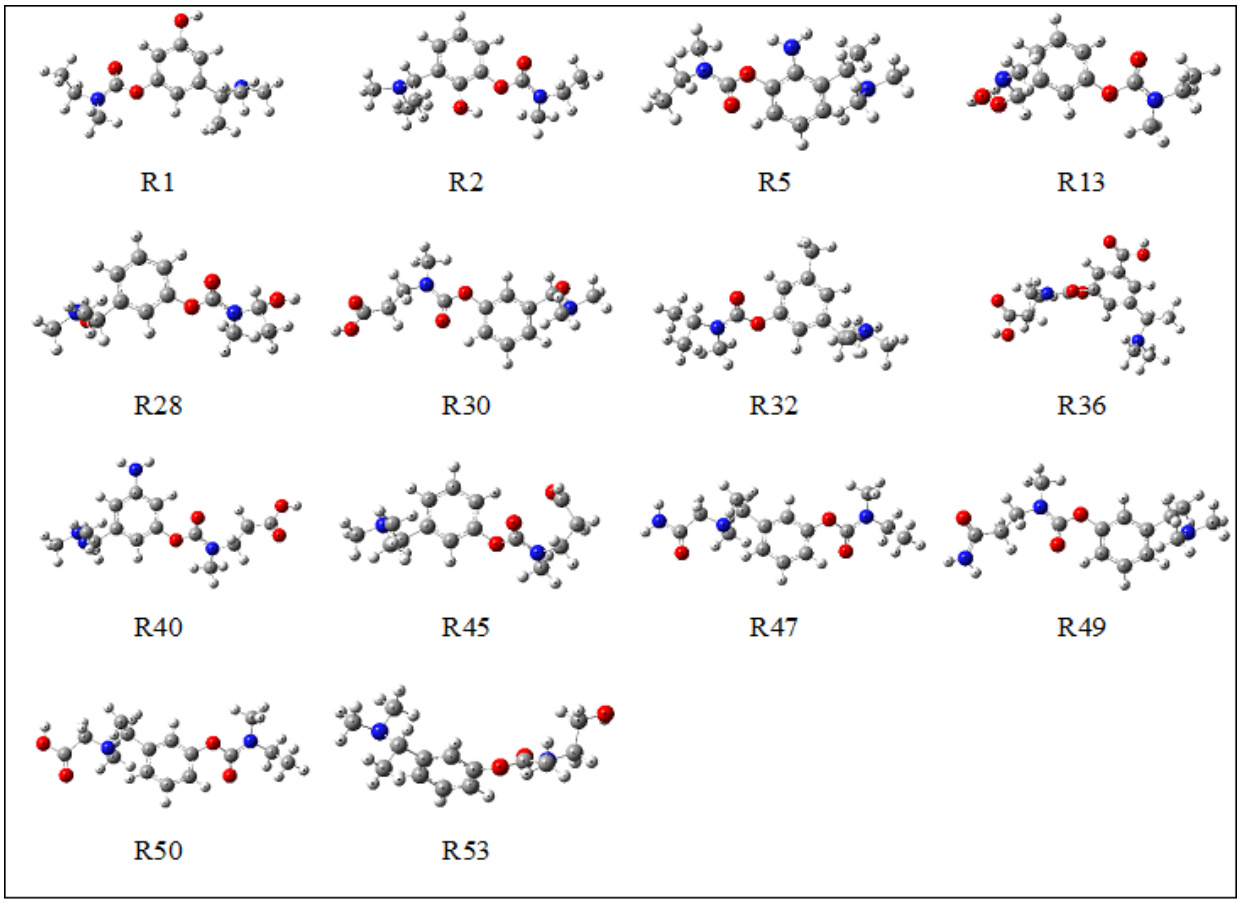

Figure 2

Best compounds having their G09 optimized structures.

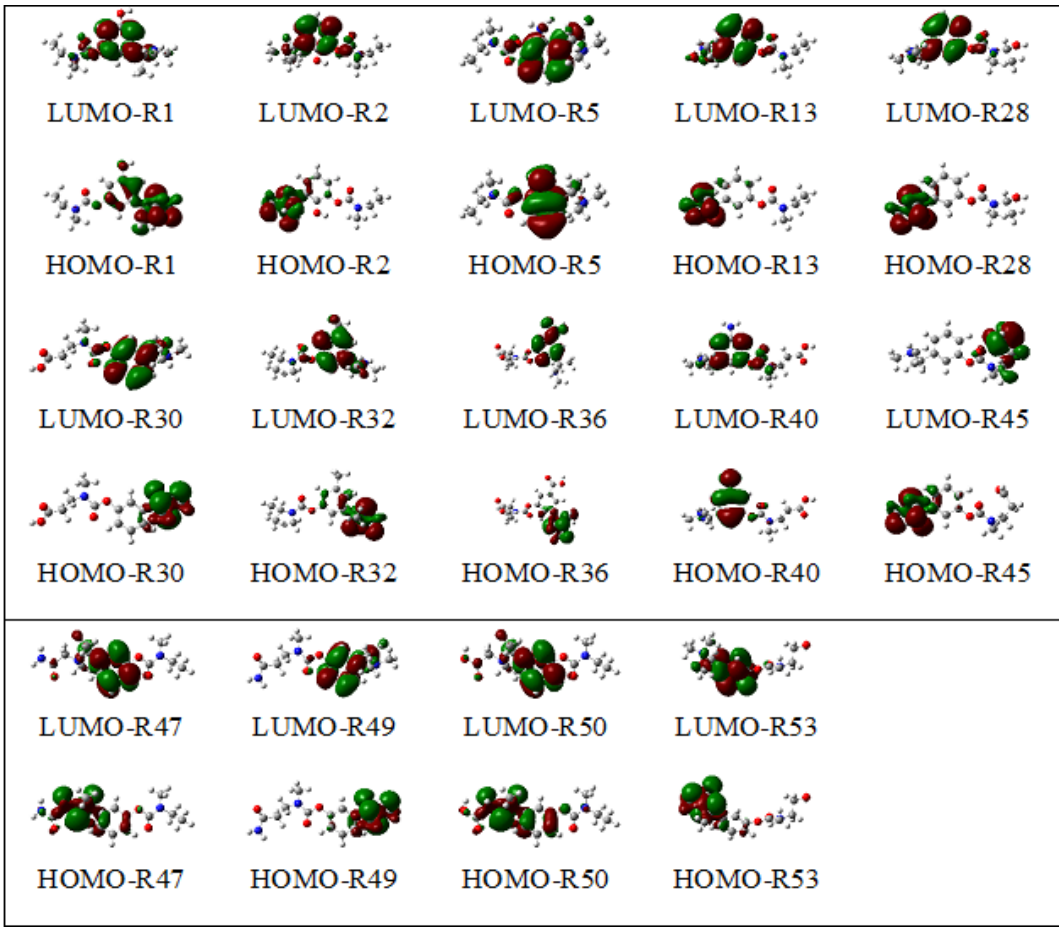

Figure 3

Contours of the occupied and unoccupied molecular orbitals of the ligands using RB3LYP/6-31G(d,p).

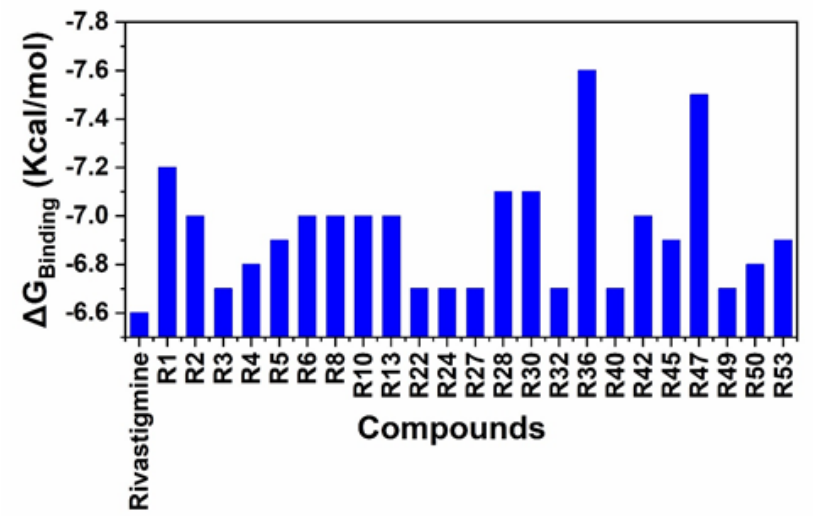

Figure 4

Comparison of binding energies of the best 23 compounds with the receptor (PDB: 4F5S).

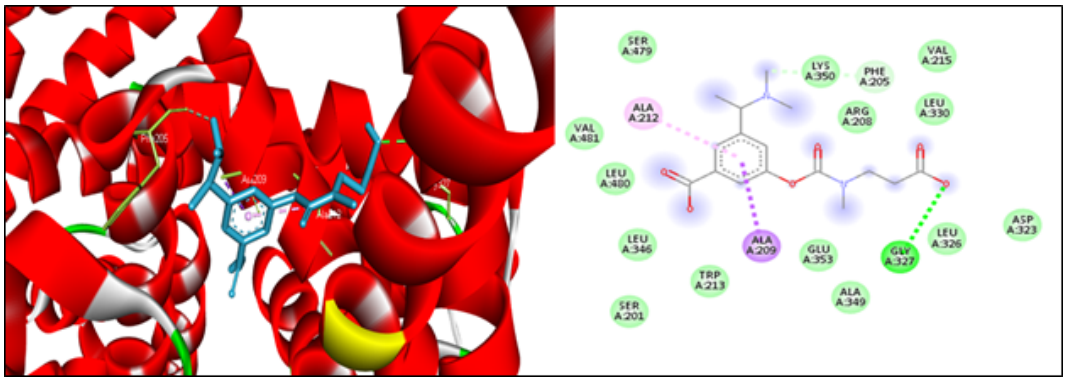

Figure 5

3D (ligands are shown as blue color) and 2D binding interaction (H- bonds are shown as green lines) of **R36** into the binding site of bovine serum albumin with PDB ID: 4F5S.

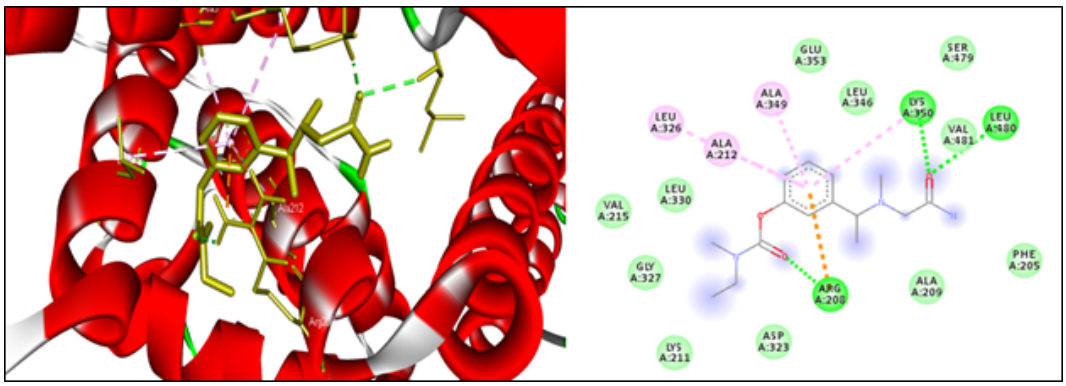

Figure 6

3D (ligands are shown as blue color) and 2D binding interaction (H- bonds are shown as green lines) of **R47** into the binding site of bovine serum albumin with PDB ID: 4F5S.

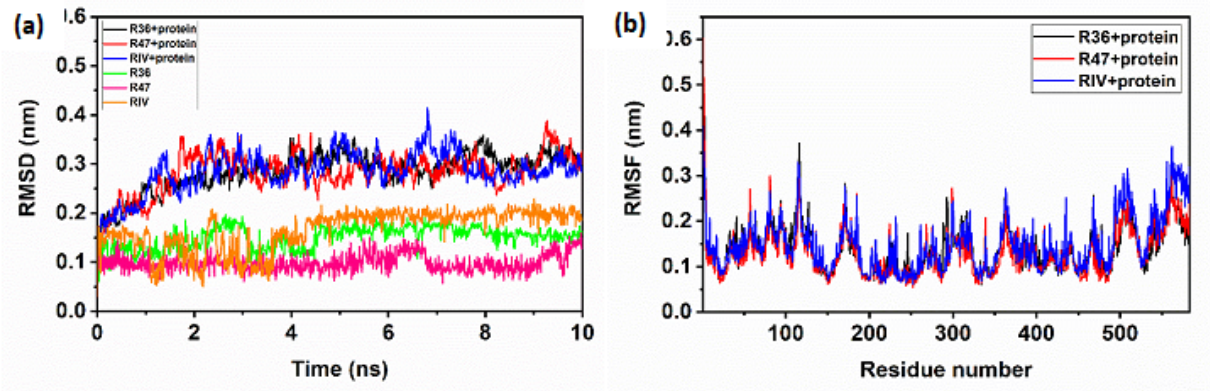

Figure 7

(a) RMSD plot of protein-ligand complexes with the receptor, (b) RMSF of all amino acids of the protein, complexes with their ligands.

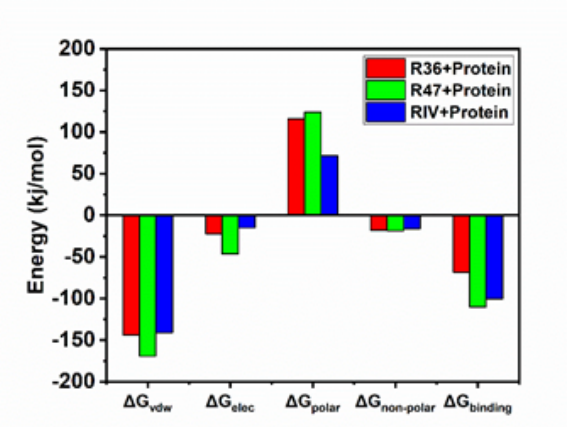

Figure 8

Different types of energies of docked ligands with the protein.

Supplementary Files

This is a list of supplementary files associated with this preprint. Click to download.

- SupplementaryRIVMCR.docx